Parkinsonism and Related Disorders 65 (2019) 146–152

Contents lists available at ScienceDirect

Parkinsonism and Related Disorders

journal homepage: www.elsevier.com/locate/parkreldis

Substantia nigra locations of iron-content, free-water and mean diffusivity abnormalities in moderate stage Parkinson's disease

Germain Arribarat[a,*], Ofer Pasternak[b], Amaury De Barros[a], Monique Galitzky[c], Oliver Rascol[a], Patrice Péran[a]

[a] ToNIC, Toulouse NeuroImaging Center, Université de Toulouse, Inserm, UPS, France
[b] Departments of Psychiatry and Radiology, Brigham and Women's Hospital, Harvard Medical School,USA
[c] Centre d'Investigation Clinique (CIC), CHU de Toulouse, Toulouse, France

ARTICLE INFO

Keywords:
Parkinson's disease
Substantia Nigra
MRI
Iron
Free-water

ABSTRACT

Background: Prior work demonstrated that free water in the posterior substantia nigra (SN) was elevated in Parkinson's disease (PD) compared to healthy controls (HC) across single- and multi-site cohorts, and increased over 1 year in Parkinson's disease but not in relation with the iron deposition in SN with the relaxometry T2*.
Objectives: The main objective of the present study was to evaluate changes in the SN using relaxometry T2*, single- and bi-tensor models of diffusion magnetic resonance imaging between PD patients and HC.
Methods: 39 subjects participated in this study, including 21 HCs and 18 PD patients, in moderate stage (7 years), whose data were collected at two visits separated by approximately 2 years, underwent 3-T MRI comprising: T2*-weighted, T1-weighted and diffusion tensor imaging (DTI) scans. Relaxometry T2*, bi-tensor free water (FW), free-water-corrected fractional anisotropy, free-water-corrected mean diffusivity, single-tensor fractional anisotropy, and single-tensor mean diffusivity were computed for the anterior, posterior and whole substantia nigra.
Results: In the anterior SN, relaxometry T2* values were greater for PD patients than HCs. In the posterior SN, free water, single- and bi-tensor mean diffusivity values were greater for PD patients than HCs. No significant change were found over time in FW/MD/R2* maps for PD patients with moderate stage.
Conclusion: The specific increase of R2* in the anterior SN concomitant with the specific increase of FW in posterior SN suggests a complementary aspect of the two parameters and, perhaps, different underlying pathophysiological processes.

1. Introduction

A key pathophysiological characteristic of Parkinson disease (PD) is the loss of the dopaminergic neurons of the substantia nigra (SN) [1], particularly in the SN pars compacta (SNc). Clinically, conventional magnetic resonance imaging (MRI) has been useful primarily for excluding underlying pathologies (e.g., vascular lesions). Because it is non-invasive and more widely available than other nuclear neuroimaging modalities, MRI has also been an advantageous technology for investigating potential biomarkers of PD onset and progression.

Postmortem histology [2] and *in vivo* MRI analyses [3] have demonstrated iron deposition in the SN of PD patients. Iron deposition can be quantitated with the T2* relaxation rate (R2*) measure in MRI data. R2* mapping studies have confirmed elevated iron content in the SN of PD patients, compared to levels in healthy controls (HCs) [3,4]. However, iron accumulation in the SN seems not to be specific to sporadic PD because it has been found in patients with multiple system atrophy as well [5,6].

Two longitudinal studies with the aim of characterizing PD progression reported conflicting R2* results among themselves. The first showed an increase SN signals [7] whereas the second failed to detect a change [8]. This discrepancy in results could be related to inconsistency in the definition of the spatial localization of the SN. Some studies have used manual segmentation of the whole SN with average markers as indices [3,5], whereas others have used manual definition of regions-of-interest (ROIs) in the SN [4,7,9,10].

Diffusion MRI sensitizes the MRI signal to the displacement of water molecules. Diffusion tensor imaging (DTI) is a popular diffusion MRI

* Corresponding author. UMR 1214, INSERM/UPS, ToNIC, Toulouse NeuroImaging Center, CHU PURPAN, Pavillon Baudot, Place du Dr Baylac, 31024, Toulouse - Cedex 3, France.
E-mail address: germain.arribarat@inserm.fr (G. Arribarat).

https://doi.org/10.1016/j.parkreldis.2019.05.033
Received 3 December 2018; Received in revised form 20 May 2019; Accepted 21 May 2019

analysis method that provides several measures including fractional anisotropy (FA), which is sensitive to the directionality of the molecule displacement, and mean diffusivity (MD), which is sensitive to molecule displacement amplitude. DTI studies have reported reduced FA of the SN in PD patients compared to HCs subjects [10,11], which may reflect the loss of dopaminergic neurons. However, a meta-analysis found no significant FA differences between PD patients and HCs in any SN regional analyses [12]. A new diffusion MRI analysis method based on the calculation of a two-tensor model has been introduced [13], wherein the fractional volume of free-water (FW) within a voxel is estimated. FW analysis has produced promising results with respect to the observation of higher values for the posterior SN in PD patients compared to HCs in single- and multi-site cohorts [14].

Both diffusion MRI and T2* relaxation studies have shown promise in differentiating PD from HCs brains. Comparison of these two sequences may help to clarify the relationship between microstructural features and iron accumulation in the SN and provide additional information regarding PD pathology. The present study is a cross-sectional and longitudinal analysis comparing T2* relaxation and diffusion MRI data, while also comparing different spatial definitions of the SN. We collected diffusion and T2* imaging data, placed them in a standard space, and compared averages of each parameter according to two different SN spatial definitions: Péran et al.'s (2010) definition employed in T2* experiments, and Vaillancourt et al.'s (2009) definition used in FW diffusion experiments. Additionally, we used a voxel-based method to investigate the SN with a data-driven approach.

2. Materials and methods

2.1. Subjects

Thirty-nine subjects participated in this study between 2014 and 2016, including 21 HCs (each individual's data were collected in a single session) and 18 PD patients, whose data were collected at two visits separated by approximately 2 years [mean interscan interval ± standard deviation (SD), 24.5 ± 4.4 months] (Table 1). PD patients were enrolled from outpatient clinics of the Toulouse PD Expert Center with the following inclusion criteria: (1) diagnosis of PD according to international diagnostic criteria [15]; (2) Hoehn and Yahr score < 4 while receiving treatment; (3) no history of neurological or psychiatric diseases other than PD; (4) no evidence of significant cognitive decline [Mini Mental State Examination score > 24 (Folstein, Folstein, & McHugh, 1975)]; (5) no deep brain stimulation treatments received; (6) no evidence of movement artifacts, vascular brain lesions, brain tumors, or marked cortical or subcortical atrophy on MRI scans. Two radiologists with substantial clinical experience examined all MRI series for the patients considered for this study to exclude any patients with potential brain abnormalities evident in conventional fluid-attenuated inversion recovery and T1-weighted images. Motor disabilities were assessed by way of Motor Examination scores of the Unified Parkinson's Disease Rating Scale (UPDRS-III). Written informed consent was obtained from all patients. This study was conducted according to the ethical principles of the Declaration of Helsinki and approved by the Toulouse Ethics Committee.

2.2. Acquisition

We used a mMRI protocol similar to our previous study [3] i.e. T1, T2 relaxometry, diffusion tensor imaging (DTI) (further details in Supplementary files).

2.3. Image analysis

Image processing was performed using FSL v5 (www.fmrib.ox.ac.uk/fsl/). Head movement parameters (rotation/translation) were estimated between Parkinson's patients and healthy subjects. FW markers and FW corrected diffusion tensor markers were calculated with a custom MATLAB R2013a code [13]. R2* markers were calculated with a custom MATLAB R2013a code [17] (for more details see Supplementary files). As a result of this processing, the FW, FA_T, FA, MD_T, MD and R2* maps were generated in the MNI space.

2.4. Spatial definition of the SN

The regions of interest (ROIs) were hand-drawn for each subject in MNI space by two trained raters, blinded to the map, subject groups, and visit.

2.4.1. Posterior and anterior SN subregions

The ROIs were hand drawn in the substantia nigra based upon the b0 images, in MNI space. The red nucleus was used as a reference because it is anatomically close to the substantia nigra and is located on the same slice as the dorsal substantia nigra. Each ROI included 8 voxels that spanned two axial slices on each image. The dorsal region contained a square ROI of four voxels (2 × 2) and the ventral ROI consisted of a square ROI of four voxels (2 × 2), based on previous work [14,18]. ROIs were drawn on the left and right anterior and posterior regions of the SN. The posterior ROIs were in voxels largely lateral to the anterior ROIs. Across subjects, the MNI coordinates for the SN ROIs were as follows: posterior right $x = -12$ to -14, $y = 20$ to 22, and $z = -10$ to -12; posterior left, $x = 10$ to 12, $y = 22$ to 24, $z = -10$ to -12; anterior right $x = -6$ to -8.0, $y = 14$ to 16, and $z = -10$ to -12; and anterior left, $x = 6.0$ to 8.0, $y = 14$ to 16, $z = -10$ to -12. **(see Fig. 1).**

2.4.2. Whole SN

The whole SN was identified as a T_2* hypo-intensity band in the midbrain, as described previously [3,5] (see Fig. 1).

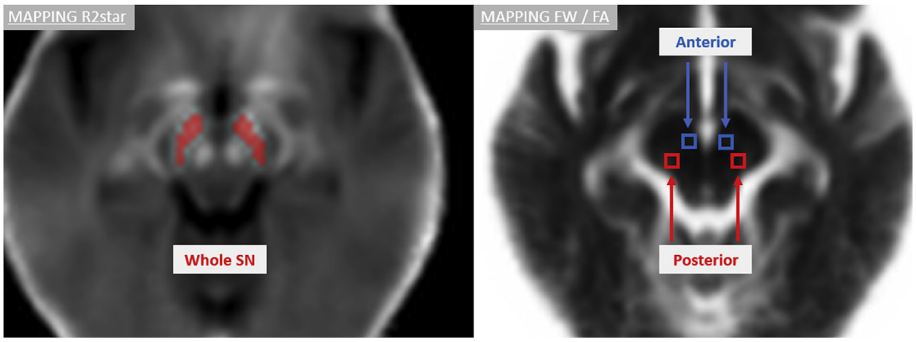

Fig. 1. On the left, an image of the iron content (R2*), with regions of interest (ROI) for the whole SN (red), for controls and Parkinson's patients.
On the right, an image in free-water (FW), with the anterior (blue) and posterior (red) ROI of the substantia nigra, for controls and Parkinson's patients.

2.4.3. Voxel-based analysis

The R_2*, MD, FA, FW, MD_T, and FA_T values were compared with a whole SN binary mask using two-sample unpaired *t*-tests. The mask was defined in the standard MNI space. This analysis was performed with the tool "randomize" from the FSL group. The number of permutations used was 5000. *P*-values (< 0.05) were corrected with the family-wise error rate method for multiple comparisons. Uncorrected *P*-values (< 0.05) were also examined.

2.5. Statistical analysis

For each subject and each ROI, we calculated mean values. We used the Shapiro-Wilk test of normality distributions to verify the appropriateness of analyzing sample means of the dependent variables (*P*-values > 0.05). To determine MRI parameter sensitivity to group differences, mean ROI values were compared between PD patients and HCs with two-sample t-tests. To determine MRI parameter sensitivity to disease progression within the PD group, mean ROI values were compared between baseline and 2-year follow-up time points with paired t-tests. For voxel-based longitudinal analysis, only MRI parameters that showed significant group differences were submitted to the analysis. To explore relationships of putative MRI markers with clinical scales, we performed multiple regression analysis for age, disease duration, Montreal Cognitive Assessment score, and UPDRS motor score for mean imaging parameter values by SN region and subregions.

3. Results

3.1. Demographic and clinical information

The participants' demographic and clinical characteristics are summarized and compared across the PD and HCs groups in Table 1. The groups were similar with respect to age and sex. From the baseline time point to the year 2 times point, MDS-UPDRS Part III scores increased significantly; no other parameters changed significantly.

3.2. ROI selection

Absolute inter- and intra-rater agreement was > 94% (kappa > 0.81, *P*-values < 0.001). No difference in head movements were found, either for rotation or translation (T2*_Rot: *P*-values = 0.13. T2*_Trans: *P*-values = 0.48; DTI_Rot *P*-values = 0.67. DTI_Trans *P*-values = 0.76), between Parkinson's patients and healthy subjects. When the SN was defined by the whole structure, PD patients displayed significantly higher R2* values than HCs, but there were no significant group differences for diffusion MRI markers (Table 2). With selection of the posterior SN, PD patients had significantly higher FW, MD, and MD_T values than HCs, but there were no significant group differences for R2*, FA, or FA_T (Table 2). With selection of the anterior SN, PD patients had significantly higher R2* values than HCs, with no significant differences for diffusion MRI markers in the anterior region (Table 2). Voxel-based analysis in the SN revealed significant R2* cluster (n = 42) (**see** Fig. 2), FW and MD cluster (n = 11 and n = 15) in the SN between the PD and HCs groups, with uncorrected p values. With corrected-p, only one significant R2* cluster (n = 11) is revealed.

Table 1
Demographic and clinical information.

	Healthy Controle (N = 21) (mean ± SD	Parkinson's Patients		*p-value*
		Baseline (N = 18) (mean ± SD)	Year 2 (N = 15) (mean ± SD)	
Age. Years	66 ± 4.91	65.2 ± 6.6	67.8 ± 7.2	–
Sex. M/F	08/13	10/08	10/05	–
Deasease duration. Month	–	82 ± 56.3	106.5 ± 60.7	–
MDS-UPDRS Part III	–	11.38 ± 4.92	17.6 ± 7.18	**0.002***
MoCA	–	28.84 ± 1.11	28.47 ± 1.18	ns
Beck Depression	–	9.94 ± 7.51	13.07 ± 8.11	ns

M = male; F = female; UPDRS-III = third part of UPDRS (Unified Parkinson's Disease Rating Scale); MoCA = Montreal Cognitive Assessment;.*ns* = not significant. Mean and SD (standard deviation) have been calculated. Significant *p-values* from T-Test are indicated in bold.

3.3. T2* versus diffusion imaging

The two SN subpart selections had different outcomes for the T2* and diffusion MRI markers. When the anterior part of the SN was defined, only the R2* data yielded significant differences between the PD and HCs groups (**see** Fig. 3). Conversely, when the posterior part of the SN was defined, several diffusion parameters (FW, MD, and MD_T) differed significantly between the PD and HCs groups (**see** Fig. 3), but there was no difference in R2*. In summary, the T2* and diffusion MRI measures produced group differences selectively for the anterior SN and posterior SN, respectively.

3.4. DTI versus FW

When the posterior SN was defined, PD patients had significantly increased FW and MD_T values compared with HCs. With conventional DTI, MD was significantly increased in the PD group relative to HCs. FA as well as FA_T did not show significant group difference.

3.5. Longitudinal analysis

The markers found to have group differences for the whole SN, or for the subregions of the SN did not significantly differ between the baseline and 2-year follow-up time points for the PD group.

3.6. MRI parameters & clinical scales

In the PD cohort, none of the baseline MRI parameters in the SN (with any kind of ROI) correlated with clinical score changes from baseline to the 2-year follow-up time point.

4. Discussion

We collected a unique dataset that allowed comparisons of iron-related and diffusion markers in the SN and thus enabled us to determine their relative sensitivities. We found that, relative to HCs, PD patients had increased R2* in the anterior SN and increased FW and MD in the posterior SN, findings suggestive of potentially distinct pathologies in the different SN subparts as well as distinct roles for these MRI markers in PD.

4.1. Diagnostic markers: the role of SN spatial definition

Our finding of increased R2* in PD patients compared to HCs in the anterior SN was confirmed in part by voxel-based analysis. An overlap between the anterior SN and the coordinates of significant voxels was obtained. The cluster found by voxel-based analysis seemed to correspond to the anterior medial SNc, in agreement with previous histochemical studies demonstrating elevated iron in PD specifically in the SNc [19,20]. One possible explanation for the detection of iron depositions in the anterior parts of the SN may be due to the absence of nigrosome degeneration in this area. The absence of partial volume with extracellular water due to the neuronal degeneration does not perturb the iron-related T2* signal. Our finding of FW increases in the posterior SN in PD patients compared to HCs is consistent with previous studies [21,22]. In addition, we found increased MD and MD_T in the

Table 2
Region of interest.

	Healthy Controle		Parkinson's Patients						PD Baseline vs Healthy Subject	PD Baseline vs PD Year 2
	N = 21		Baseline (N = 18)		Baseline (N = 15)		Year 2 (N = 15)		*p-value*	*p-value*
	Mean	DS	Mean	SD	Mean	SD	Mean	SD		
Posterior SN R2star	25.02	2.14	25.96	3.12	26.01	3.36	26.66	3.09	ns	ns
Posterior SN FW	**10.99**	4.52	**15.65**	4.93	**14.97**	4.78	**15.13**	3.53	**0.004****	**ns**
Posterior SN FA	4578.55	564.03	4426.59	554.56	4473.69	575.53	4378.7	322.27	ns	ns
Posterior SN MD	**673.32**	78.93	**744.00**	79.48	**730.68**	77.36	**732.52**	74.91	**0.008****	**ns**
Posterior SN FA_T	5160.39	522.75	5249.99	450.03	5266.06	472.55	5170.30	295.67	ns	ns
Posterior SN MD_T	**538.41**	29.23	**557.75**	29.05	**551.62**	27.97	**551.41**	30.79	**0.04***	**ns**
Anterior SN R2star	**27.26**	2.97	**31.05**	3.61	**31.43**	3.74	**31.72**	3.86	**0.001****	**ns**
Anterior SN FW	11.82	4.86	11.81	3.35	11.59	3.27	12.68	6.01	ns	ns
Anterior SN FA	4231.21	567.08	4219.16	417.12	4166.63	376.65	4059.95	419.43	ns	ns
Anterior SN MD	648.68	93.25	652.28	77.35	646.30	78.48	656.23	100.18	ns	ns
Anterior SN FA_T	4754.59	486.26	4706.70	394.66	4644.42	346.58	4602.45	300.55	ns	ns
Anterior SN MD_T	499.10	43.81	501.54	42.37	498.44	45.34	491.96	25.99	ns	ns
Whole SN R2star	**29.96**	2.97	**34.47**	3.03	**34.74**	3.27	**35.81**	3.33	< **0.001*****	**ns**
Whole SN FW	12.17	4.19	12.99	2.28	12.14	2.40	12.67	2.50	ns	ns
Whole SN FA	4520.67	388.71	4470.71	360.34	4388.07	310.21	4413.88	240.69	ns	ns
Whole SN MD	668.57	77.13	672.37	50.18	669.72	53.38	657.83	41.21	ns	ns
Whole SN FA_T	5123.94	377.30	5126.74	381.99	5040.17	331.30	5032.79	205.39	ns	ns
Whole SN MD_T	506.66	28.40	502.33	28.13	497.10	27.27	491.03	16.39	ns	ns

R2*: s^{-1}; MD: ($\times 10^{-3}$ mm^2/s). The variables are multiplied (x10 - FW, x1000 – MD and MD_T, x10000 – FA and FA_T) for a better statistical representation. All values correspond to the mean values of ROI. SD = Standard Deviation. *ns* = not significant. Significant *p-values* are indicated in bold (**:p < 0.01; ***:p < 0.001).

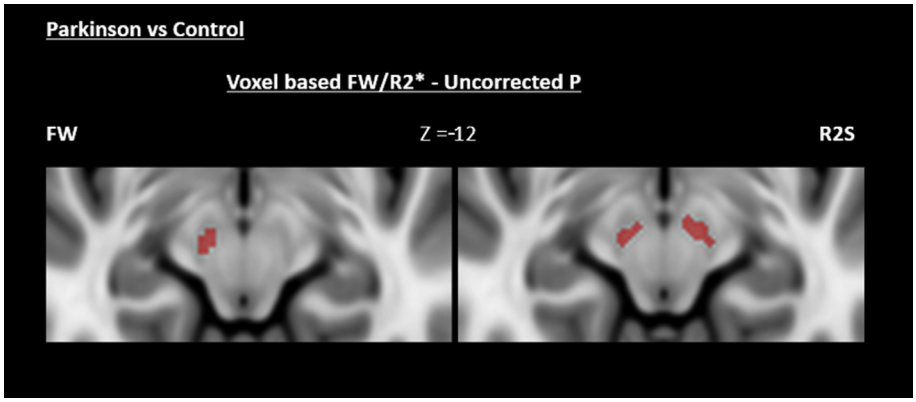

Fig. 2. Differences between patients with Parkinson's disease and controls from voxel-based analysis of R_2*, for the substantia nigra location.

posterior SN of PD patients. As demonstrated by Mishra et al., 2015, FW can be linearly mapped to MD and could explain both extracellular and cellular changes [23]. The location of posterior SN appears to correspond to the location of the nigrosome-1 [24]. Its absence could explain the increase of FW and MD.

FW identifying atrophy/cellular deterioration, versus T2* identifying iron depositions. The specific increase of R2* in the anterior SN concomitant with the specific increase of FW in posterior SN suggests a complementary aspect of the two parameters and, perhaps, different underlying pathophysiological processes. This potential complementarity is not surprising considering previous interpretations of PD-related changes wherein SN R2* increases are classically interpreted as increased iron content due to neurotoxicity [25], while FW and MD increases are classically interpreted as a rarefaction of the cells [14,22].

The role of SN spatial definition is crucial for PD, particularly for SNc. At the time of the onset of PD symptoms, a significant portion of neurons containing neuromelanin (NM) were lost. Iron deposition occurs at the same time as this loss. T2/T2*-weighted images are not sensitive to NM and therefore localization of the SNc. Neuromelanin-sensitive MRI (MRI-NM) can generate a contrast to NM [26,27]. Some studies have demonstrated that the SN observed in T2/T2* contrasts is spatially non-conform to the NM-MRI [28]. The T2/T2* sequences, should be spatially correlated with the NM-MRI, to assess the potential impact of neuromelanin and its potential role in iron disease mechanisms, particularly in a sub-regional approach. When SNpc is defined by neuromelanin-sensitive MRI, Langley et al. showed that the mean value of R2* is significantly increased in PD [29]. We assume that in the future, it will be interesting to compare the topographic aspect of the R2*/MD/FW biomarkers studied in SN of patients with intermediate PD with neuro-melanin imaging.

4.2. Disease progression marker

We found no significant change over time in FW/MD/R2* maps in patients with PD, despite the use of different ROI types to describe the SN. Our lack of significant changes over time could be a ceiling effect for iron content due to advanced disease stage. Indeed, our PD patient group had a disease duration of about 7 years on average, a duration corresponding to advanced PD. The current findings are consistent with Guttuso et al. [30], with a baseline mean idiopathic Parkinson disease duration of 7.1 years. Hopes et al. (2016) observed R2* changes in the SN over 2 years in early-stage PD patients, but this same study did not show differences in SN R2* when early and advanced patient were analyzed together, consistent with the ceiling effect interpretation. R2* in the anterior SN and FW in the posterior SN seem to be sensitive enough to detect cross-sectional differences (PD patients versus HCs)

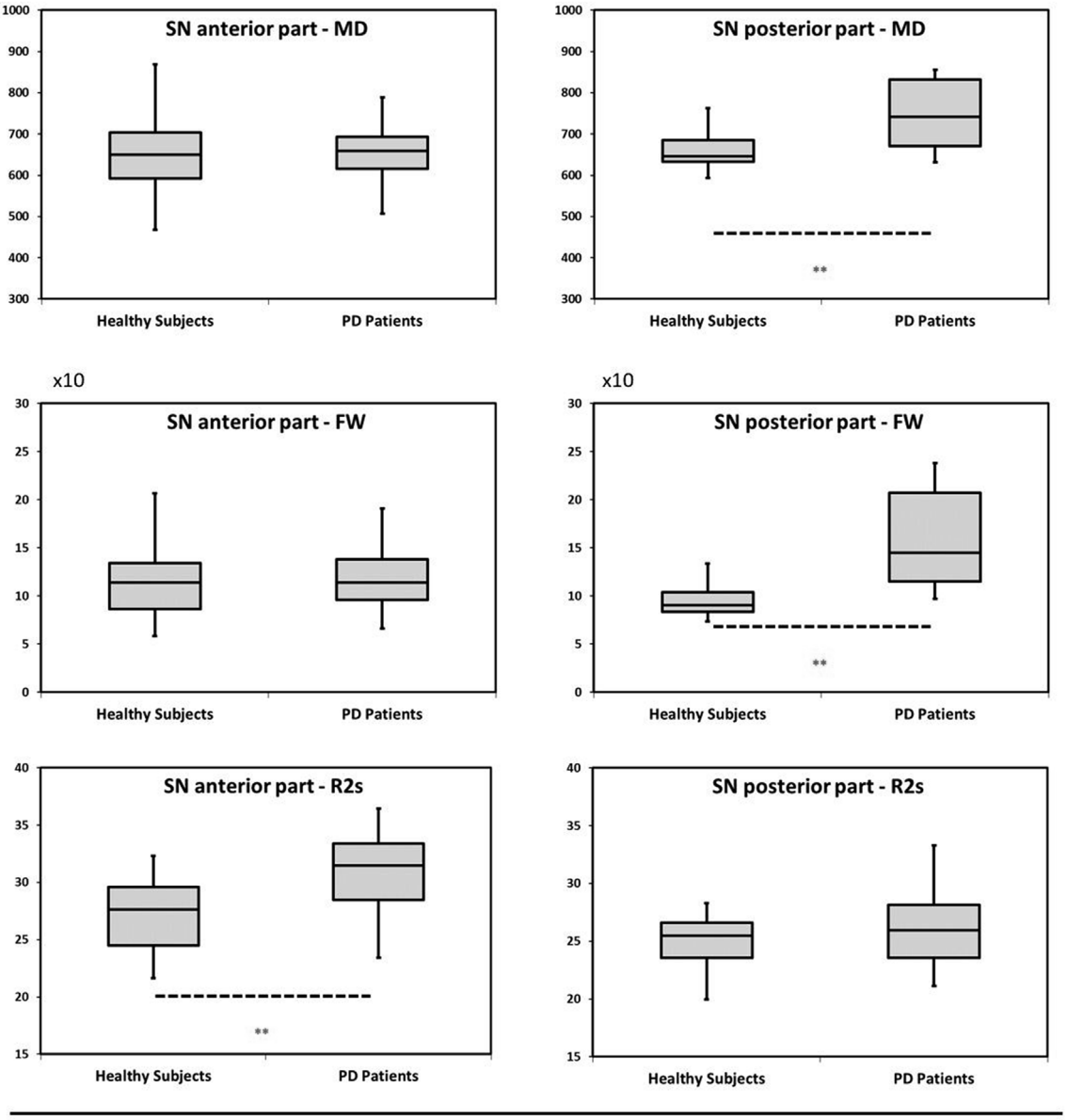

**: p<0.01. R2*: s^{-1}; MD: (× 10^{-3} mm^2/s). The variables are multiplied for a better statistical representation.

Fig. 3. Mean group values for free-water, mean diffusivity and R2* of the anterior (left) and posterior (right) SN.

but not to detect progression in advanced PD patients. The prior free-water longitudinal findings [21] were observed in early stage PD with a different cohort, which was not the case of the present study. In addition, this prior work showing longitudinal free-water changes in early PD has been replicated in the Parkinson's Progression Markers Initiative (PPMI) cohort in early stage PD [32]. In addition, other groups have also found FA changes longitudinally in the substantia nigra in early stage PD [33].

Previous data have demonstrated changes in SN pigmentation and iron deposition with healthy aging [18]. Therefore, a longitudinal evaluation of PD appears to require simultaneous evaluation of the same imaging sequences in HC, particularly for early stage evaluation of the disease. With this approach, the inclusion of an atypical cohort would allow comparison of imaging methods based on R2*/diffusion measurements for SN, in the anterior and posterior parts.

The lack of longitudinal change sensitivity could be also explained by a relative high-resolution acquisition using in this current study compared to previous studies (e.g. FW: [21]; T2*: [3]) that decrease signal on noise ratio. In addition, diffusion multi-shell acquisitions are preferred to obtain bi-tensor fit more stable [23].

4.3. MRI markers of PD-related SN pathophysiology

Gerlach, Double, Youdim, and Riederer (2006) proposed several hypotheses to explain iron accumulation in the SN of PD patients, including increased iron in dopaminergic neurons as well as microglial activation, which may be undetectable at an advanced stage. This hypothesis is aligned with our results and with Devos' research group's study [31] demonstrating a lack of longitudinal R2* changes in advanced PD patients and a lack R2* differences between early and advanced patients. Even if R2* is not specific to only one iron-bound protein [34], the R2* relaxometry method has convincing histochemical results in postmortem brain tissue studies [2].

Pasternak and colleagues have demonstrated that FW mapping

provides some information about tissue microstructure, including changes related to atrophy, neuroinflammation, and cellular density [30]. This increase, in the SN posterior parts, has been interpreted as cell rarefaction, an interpretation which can also explain concomitant MD increases. This delineation of the SN may correspond to the dorsolateral SNc, a site of dopaminergic neuron degeneration.

Cross-sectional analysis of diffusion MRI and T2* markers did not reveal a relationship of R2* or FW values in the SN with motor deficit. This lack of a correlation between MRI markers and direct indexes of clinical disability (UPDRS-III score) in the PD group may be due to the patients being assessed while on dopaminergic medications alleviating their symptoms [3,31,35]. The aforementioned ceiling effect in advanced PD patients could also help to explain the lack of correlation.

A potential limitation of this study could be the number of patients included. Our monocentric longitudinal study makes it difficult to recruit a large cohort of PD patients but enables us to avoid confounding factors related to multicenter studies (e.g., center and sequence effects). The study design was appropriate for confirming previously highlighted results and evaluating the different SN definitions with a variety of imaging markers. Secondly, our study investigated advanced PD patients on medication. Longitudinal studies on *de novo* untreated PD patients will be crucial to confirming the potential utility of R2*/MD/FW markers for diagnosis and disease progression monitoring. The possibility of a larger cohort will also clarify the relationship between the sexes regarding the deposition and metabolism of iron in the brain, particularly over time. Also, it would be interesting to include a longitudinal group of HC to assess physiological variability and a better appreciation of the biomarker topography.

5. Conclusion

The specific increase in R2* in the anterior SN concomitant with the specific increase in FW in the posterior SN suggests a complementary aspect of the two parameters and, possibly, different underlying pathophysiological processes. The boundaries between SNr and SNc are difficult to define, due to the groups of SNc neurons deeply embedded in the SNr. The small size of the SNr and its position make it difficult to obtain a clear image with current methods. These results demonstrate the need for high resolution imaging in the substantia nigra allowing the distinction of new patients with Parkinson's disease (PD) at an early stage from healthy individuals.

Specific image processing techniques, such as noise reduction and super-resolution reconstruction, can improve image quality. Finally, with the possibility of obtaining phase imaging without adding time acquisition, it could be interesting to compare a multi-contrast acquisition collection (R2*/QSM/SWI) with multishell diffusion imaging and neuromelanin-sensitive imaging data.

Authors' roles

1. Research Project: A. Conception, B. Organization, C. Execution; 2. Statistical Analysis: A. Design, B. Execution, C. Review and Critique; 3. Manuscript Preparation: A. Writing the First Draft, B. Review and Critique.

G.A.: 2AB, 3A
O.P.: 2ABC, 3B
A.D.B.:3B
M.G.:1C.
O.R.:1ABC, 2 C, 3B
P.P.: 1ABC, 2ABC, 3B

Financial disclosures of all authors

Germain Arribarat: Nothing to report.
Ofer Pasternak: Nothing to report.
Monique Galitzky: Nothing to report.

Olivier Rascol has received research grants from the CHU de Toulouse, France-Parkinson, INSERM-DGOS (the Translational Research program), the French Ministry of Health (the PHRC program), Lundbeck, TEVA and UCB. He has served on advisory boards, served as a consultant and given lectures for pharmaceutical companies such as Abbott, Addex, BIAL, Boehringer-Ingelheim, Impax Pharmaceuticals, Lundbeck, Merck, Merck-Serono, Novartis, Oxford Biomedica, TEVA, UCB, and Xenoport.

Patrice Péran: Nothing to report.

Conflicts of interest

Nothing to report.

Funding sources

The study was sponsored by Inserm and funded by a “Recherche clinique translationnelle” grant from INSERM-DGOS (2013–2014).

Acknowledgments

This study was supported by a “Recherche clinique translationnelle” grant from INSERM-DGOS 2013–2014. We thank the Center d’Investigation Clinique (CIC) for the global coordination of the clinical study and the Inserm/UPS UMR1214 Technical Platform for the MRI acquisitions.

Appendix A. Supplementary data

Supplementary data to this article can be found online at https://doi.org/10.1016/j.parkreldis.2019.05.033.

References

[1] P. Damier, E.C. Hirsch, Y. Agid, A.M. Graybiel, The substantia nigra of the human brain. II. Patterns of loss of dopamine-containing neurons in Parkinson's disease, Brain 122 (Pt 8) (Aug. 1999) 1437–1448.
[2] A. Galvan, T. Wichmann, Pathophysiology of parkinsonism, Clin. Neurophysiol. 119 (7) (Jul. 2008) 1459–1474.
[3] P. Péran, et al., Magnetic resonance imaging markers of Parkinson's disease nigrostriatal signature, Brain 133 (11) (2010) 3423–3433.
[4] W.R.W. Martin, M. Wieler, M. Gee, W.H. Oertel, P. Boesiger, M. Anliker, Midbrain iron content in early Parkinson disease: a potential biomarker of disease status, Neurology 70 (16 Pt 2) (Apr. 2008) 1411–1417.
[5] G. Barbagallo, et al., Multimodal MRI assessment of nigro-striatal pathway in multiple system atrophy and Parkinson disease, Mov. Disord. 31 (3) (2016) 325–334.
[6] P. Péran, et al., MRI supervised and unsupervised classification of Parkinson's disease and multiple system atrophy, Mov. Disord. 33 (4) (Apr. 2018) 600–608.
[7] M. Ulla, J.M. Bonny, L. Ouchchane, I. Rieu, B. Claise, F. Durif, Is R2* a new MRI biomarker for the progression of Parkinson's disease? A longitudinal follow-up, PLoS One 8 (3) (2013) e57904.
[8] M. Wieler, M. Gee, W.R.W. Martin, Longitudinal midbrain changes in early Parkinson's disease: iron content estimated from R2*/MRI, Park. Relat. Disord. 21 (3) (Mar. 2015) 179–183.
[9] G. Du, et al., Distinct progression pattern of susceptibility MRI in the Substantia Nigra of Parkinson's Patients, Mov. Disord. (May 2018).
[10] D.E. Vaillancourt, et al., High-resolution diffusion tensor imaging in the substantia nigra of de novo Parkinson disease, Neurology 72 (16) (Apr. 2009) 1378–1384.
[11] S. Lehéricy, M.A. Sharman, C.L. Dos Santos, R. Paquin, C. Gallea, Magnetic resonance imaging of the substantia nigra in Parkinson's disease, Mov. Disord. 27 (7) (Jun. 2012) 822–830.
[12] S.T. Schwarz, M. Abaei, V. Gontu, P.S. Morgan, N. Bajaj, D.P. Auer, Diffusion tensor imaging of nigral degeneration in Parkinson's disease: a region-of-interest and voxel-based study at 3 T and systematic review with meta-analysis, NeuroImage. Clin. 3 (2013) 481–488.
[13] E. Ofori, et al., Free water improves detection of changes in the substantia nigra in parkinsonism: a multisite study, Mov. Disord. 32 (10) (2017) 1457–1464.
[14] E. Ofori, et al., Increased free water in the substantia nigra of Parkinson's disease: a single-site and multi-site study, Neurobiol. Aging 36 (2) (2015) 1097–1104.
[15] A.J. Hughes, S.E. Daniel, L. Kilford, A.J. Lees, Accuracy of clinical diagnosis of idiopathic Parkinson's disease: a clinico-pathological study of 100 cases, J. Neurol. Neurosurg. Psychiatry 55 (3) (1992) 181–184.
[17] P. Péran, et al., Voxel-based analysis of R2* maps in the healthy human brain, J. Magn. Reson. Imaging 26 (6) (Dec. 2007) 1413–1420.

[18] D.E. Vaillancourt, M.B. Spraker, J. Prodoehl, X.J. Zhou, D.M. Little, Effects of aging on the ventral and dorsal substantia nigra using diffusion tensor imaging, Neurobiol. Aging 33 (1) (2012) 35–42.
[19] S. Ayton, P. Lei, Nigral iron elevation is an invariable feature of Parkinson's disease and is a sufficient cause of neurodegeneration, BioMed Res. Int. (2014) 581256 Jan. 2014.
[20] D.T. Dexter, et al., Alterations in the levels of iron, ferritin and other trace metals in Parkinson's disease and other neurodegenerative diseases affecting the basal ganglia, Brain 114 (Pt 4) (Aug. 1991) 1953–1975.
[21] E. Ofori, et al., Longitudinal changes in free-water within the substantia nigra of Parkinson's disease, Brain 138 (8) (Aug. 2015) 2322–2331.
[22] P.J. Planetta, et al., Free-water imaging in Parkinson's disease and atypical parkinsonism, Brain 139 (2) (2016) 495–508.
[23] V. Mishra, X. Guo, M.R. Delgado, H. Huang, Toward tract-specific fractional anisotropy (TSFA) at crossing-fiber regions with clinical diffusion MRI, Magn. Reson. Med. 74 (6) (Dec. 2015) 1768–1779.
[24] A.I. Blazejewska, et al., Visualization of nigrosome 1 and its loss in PD: pathoanatomical correlation and in vivo 7 T MRI, Neurology 81 (6) (Aug. 2013) 534–540.
[25] L. Zecca, M.B.H. Youdim, P. Riederer, J.R. Connor, R.R. Crichton, Iron, brain ageing and neurodegenerative disorders, Nat. Rev. Neurosci. 5 (11) (Nov. 2004) 863–873.
[26] P. Trujillo, et al., Contrast mechanisms associated with neuromelanin-MRI, Magn. Reson. Med. 78 (5) (Nov. 2017) 1790–1800.
[27] D. Sulzer, et al., Neuromelanin detection by magnetic resonance imaging (MRI) and its promise as a biomarker for Parkinson's disease, npj Park. Dis. 4 (1) (Dec. 2018) 11.
[28] S. Lehéricy, E. Bardinet, C. Poupon, M. Vidailhet, C. François, 7 tesla magnetic resonance imaging: a closer look at substantia nigra anatomy in Parkinson's disease, Mov. Disord. 29 (13) (Nov. 2014) 1574–1581.
[29] J. Langley, N. He, D.E. Huddleston, S. Chen, F. Yan, B. Crosson, X. Hu, et al., Reproducible detection of nigral iron deposition in 2 Parkinson's disease cohorts, Mov. Disord (2018), https://doi.org/10.1002/mds.27608.
[30] T. Guttuso, N. Bergsland, J. Hagemeier, D.G. Lichter, O. Pasternak, R. Zivadinov, Substantia nigra free water increases longitudinally in Parkinson disease, Am. J. Neuroradiol., Feb. (2018), https://doi.org/10.3174/ajnr.A5545.
[31] L. Hopes, et al., Magnetic resonance imaging features of the nigrostriatal system: biomarkers of Parkinson's disease stages? PLoS One 11 (4) (2016) e0147947.
[32] R.G. Burciu, et al., Progression marker of Parkinson's disease: a 4-year multi-site imaging study, Brain 140 (8) (Aug. 2017) 2183–2192.
[33] C. Loane, et al., Aberrant nigral diffusion in Parkinson's disease: a longitudinal diffusion tensor imaging study, Mov. Disord. 31 (7) (Jul. 2016) 1020–1026.
[34] M. Gerlach, K.L. Double, M.B.H. Youdim, P. Riederer, Potential sources of increased iron in the substantia nigra of parkinsonian patients, J. Neural Transm. Suppl. (70) (2006) 133–142.
[35] G. Du, et al., Imaging nigral pathology and clinical progression in Parkinson's disease, Mov. Disord. 27 (13) (Nov. 2012) 1636–1643.